Genomic loss of the putative tumor suppressor gene *E2A* in human lymphoma

Anne Steininger,[1] Markus Möbs,[2] Reinhard Ullmann,[1] Karl Köchert,[4] Stephan Kreher,[4] Björn Lamprecht,[4] Ioannis Anagnostopoulos,[3] Michael Hummel,[3] Julia Richter,[5] Marc Beyer,[2] Martin Janz,[4] Claus-Detlev Klemke,[6] Harald Stein,[3] Bernd Dörken,[4] Wolfram Sterry,[2] Evelin Schrock,[7] Stephan Mathas,[4] and Chalid Assaf[2,8]

[1]Max Planck Institute for Molecular Genetics, 14195 Berlin, Germany
[2]Department of Dermatology and Allergy, Skin Cancer Center Charité, [3]Institute of Pathology, Charité-Universitätsmedizin Berlin, 10117 Berlin, Germany
[4]Hematology, Oncology and Tumorimmunology, Charité-Universitätsmedizin Berlin and Max-Delbrück-Center for Molecular Medicine, 13125 Berlin, Germany
[5]Institute of Human Genetics, Christian-Albrechts-University Kiel and University Hospital Schleswig-Holstein, Campus Kiel, 24105 Kiel, Germany
[6]Department of Dermatology, University Medical Center Mannheim, Ruprecht-Karls-University of Heidelberg, 68167 Mannheim, Germany
[7]Institute for Clinical Genetics, Dresden University of Technology, 01307 Dresden, Germany
[8]HELIOS Klinikum Krefeld, 47805 Krefeld, Germany

The transcription factor E2A is essential for lymphocyte development. In this study, we describe a recurrent *E2A* gene deletion in at least 70% of patients with Sézary syndrome (SS), a subtype of T cell lymphoma. Loss of *E2A* results in enhanced proliferation and cell cycle progression *via* derepression of the protooncogene *MYC* and the cell cycle regulator *CDK6*. Furthermore, by examining the gene expression profile of SS cells after restoration of E2A expression, we identify several E2A-regulated genes that interfere with oncogenic signaling pathways, including the Ras pathway. Several of these genes are down-regulated or lost in primary SS tumor cells. These data demonstrate a tumor suppressor function of E2A in human lymphoid cells and could help to develop new treatment strategies for human lymphomas with altered E2A activity.

CORRESPONDENCE
Chalid Assaf:
chalid.assaf@charite.de
OR
Stephan Mathas:
stephan.mathas@charite.de

Abbreviations used: AAD, aminoactinomycin D; CGH, comparative genomic hybridization; EMSA, electrophoretic mobility shift assay; FISH, fluorescence in situ hybridization; SS, Sézary syndrome.

E-proteins define a distinct class of basic helix-loop-helix transcription factors that are central regulators of cellular differentiation in various cell types and are essential for the development of B and T lymphocytes (Kee, 2009). There are three known E-protein coding genes in mammals, namely *E2A* (also called *TCF3*), *E2-2* (also called *TCF4*) and *HEB* (HeLa E-box binding protein; also called *TCF12*), which all bind to a DNA sequence motif called E-box (CANNTG). The *E2A* gene, which is located on chromosome 19p13.3, encodes for two different basic helix-loop-helix transcription factors, E12 and E47, which are generated by alternative splicing (Mellentin et al., 1989; Murre et al., 1989). E2A proteins form homodimers and heterodimers with other HLH proteins to conduct their tissue- or cell type–specific functions (Kee, 2009).

Alterations of E2A expression and activity have been suggested to support malignant transformation of lymphoid cells. In mice, deletion of *E2A*, as well as enforced expression of its inhibitors, e.g., the inhibitor of DNA binding (Id) proteins, lead to rapid development of aggressive T cell lymphomas and T cell hyperproliferations (Bain et al., 1997; Yan et al., 1997; Morrow et al., 1999). In humans, diminished E2A activity has been proposed as a pathogenetic mechanism in TAL1/SCL- or E2A-PBX1–induced leukemias (Park et al., 1999; Aspland et al., 2001; O'Neil et al., 2004), and functional blockade of E2A is involved in

A. Steininger and M. Möbs contributed equally to this paper.
S. Mathas and C. Assaf contributed equally to this paper.

The Rockefeller University Press $30.00
J. Exp. Med. Vol. 208 No. 8 1585-1593
www.jem.org/cgi/doi/10.1084/jem.20101785

the pathogenesis of human lymphomas (Mathas et al., 2006, 2009; Lietz et al., 2007). However, a frequent genomic loss of *E2A* has not been identified in human lymphoid malignancies so far. Arguing for a function as tumor suppressor in human cells, our study now demonstrates a recurrent deletion of *E2A* in leukemic cells of patients suffering from Sézary syndrome (SS), an aggressive variant of primary cutaneous T cell lymphoma characterized by the presence of neoplastic T cells in skin, lymph nodes, and peripheral blood (Willemze et al., 2005).

RESULTS AND DISCUSSION

In a genome-wide analysis of peripheral blood mononuclear cells from 20 SS patients (Table S1) by array comparative genomic hybridization (array CGH), we identified a minimal common region of chromosomal loss on chromosome 19p13.3 in 70% (14/20) of patients (Fig. 1 A, Table I, Fig. S1, and Table S2). This region of ~1.4 Mb ranging from chr19:1368087 to chr19:2824434 (HG18) included the *E2A* gene locus. Fluorescence in situ hybridization (FISH) analysis on highly enriched tumor cells using an *E2A*-specific probe confirmed a heterozygous loss of *E2A* in 8/12 analyzed SS patient samples (Fig. 1 B and Table I; for details on tumor cell enrichment see Materials and methods, Fig. S2, and Table S3). The number of cases with *E2A* deletion might even be underestimated because in two cases without deletion in array CGH analysis, a deletion of *E2A* was detected by FISH (Table I). Concomitant with the genomic loss of *E2A*, the *E2A* mRNA expression level in enriched leukemic cells of SS patients was significantly reduced compared with purified $CD4^+$ T cells from healthy volunteers (Fig. 1 C and Fig. S3 A; note, that the ΔCt of *E12/E47* or *E47*, respectively, is significantly lower in $CD4^+$ controls compared with SS patient samples. Hence, relative to *GAPDH*, SS patient samples express less *E12/E47* or *E47* mRNA, respectively, than the control $CD4^+$ T lymphocytes), and immunohistochemistry showed weak or absent E2A protein expression in skin-infiltrating tumor cells in 15/15 patient samples (Fig. 1 D).

Among cutaneous T cell lymphomas, SS is unique in respect to the presence of a high load of lymphoma cells in the peripheral blood. Because E2A interferes with cell cycle control (Park et al., 1999; Murre, 2005), we first investigated the impact of reduced *E2A* expression on the growth of malignant SS cells. To this end, we chose the SS-derived Se-Ax cell line, which is associated with a heterozygous loss of *E2A* (Fig. 1 B and Table I) and is characterized by reduced E2A mRNA and protein levels and impaired E-box DNA binding activity (Fig. 1, E and F and Fig. S3 B). After transient transfection with a Myc-tagged E47 construct and, alternatively, a construct coding for two covalently linked E47 molecules (E47-forced dimer, E47-FD), Se-Ax cells showed a pronounced reduction of proliferation (Fig. 2 A). No significant effect on apoptosis induction was observed (unpublished data). To prove the biological significance of our transfection approach, we investigated transgene expression as well as the resulting E2A-DNA binding activity by immunoblotting and electrophoretic mobility shift assay. In both analyses, we reached levels comparable to endogenous ones in other T cell leukemia–derived cell lines (Fig. S3 C). To substantiate our finding of reduced proliferation after E2A reconstitution, we measured DNA synthesis (determined by BrdU incorporation) and the respective cell cycle phases (determined by 7-aminoactinomycin D [7-AAD] staining) in parallel by a two-color flow cytometric analysis (Fig. 2 B). This experimental approach revealed that reexpression of E2A in Se-Ax cells significantly increased the fraction of cells in the G0/G1 phase at the expense of cells in the S phase of the cell cycle, suggesting that the reduced proliferation of Se-Ax cells after E2A reconstitution is caused by a G0/G1 cell cycle arrest.

To establish a mechanistic link between E2A reduction and deregulated cell cycle control, we analyzed mRNA expression of the protooncogene *MYC* and the cell cycle regulator *CDK6* in Se-Ax cells. After E2A reconstitution, we observed significantly reduced mRNA levels of both genes (Fig. 2 C), suggesting a pathogenetically relevant link in these human T cell–derived lymphoma cells. In line with these in vitro data, we observed robust protein expression of CDK6 in 7 out of 7 and, in accordance with previously published data (Vermeer et al., 2008), of MYC in 5 out of 6 primary SS tumor samples (Fig. 2 D). The high level of MYC expression in the SS tumor cells is in the majority of our SS cases most likely supported by genomic gains of chromosome 8q, which also includes the *MYC* locus (Fig. S1 and Table S4). Notably, the MYC-induced apoptotic program (Eischen et al., 1999) might be counteracted by the loss of 17p, including the tumor suppressor gene *TP53,* as demonstrated in a large number of our SS patient samples (Table S4).

To further investigate the impact of diminished E2A expression on SS tumor cells, we characterized E2A-dependent transcriptional changes in Se-Ax cells by microarray gene expression analyses. A highly overlapping, limited number of genes were responsive to E2A reconstitution with either E47 or E47-FD (Fig. S3 D and Table S5). Overall, far more genes were induced than repressed. Arguing for the biological relevance of our microarray analyses, the E2A-regulated genes in our data showed a significant overlap with E2A-dependent genes identified in *E2A*-deficient murine T cell lymphoma (Schwartz et al., 2006) and in a murine *E2A*-deficient hematopoietic progenitor cell line (Ikawa et al., 2006; Fig. S3 E and Table S6). In our dataset, among the E2A-induced genes were proapoptotic genes like *BCL2L11* and *BIK*, genes known to modulate T cell–specific signaling pathways and differentiation (*DTX1*, *MAL*), as well as negative regulators of oncogenic signaling pathways including the Ras signaling pathway (*RASSF4*, *DAB2IP*, *RASA4*, *RGS16*). The E2A-dependent up-regulation of these genes was confirmed by quantitative PCR (Fig. 3 A). In view of their dependency on E2A, expression would be expected to be down-regulated or lost in SS tumor cells because of their reduced *E2A* expression. Accordingly, *BCL2L11* and *MAL* were previously described to be specifically down-regulated in SS cells (Kari et al., 2003; van Doorn et al., 2004). In our samples, *BCL2L11*, *DTX1*, and *RASSF4* were found to be down-regulated in 4/4 of our SS patient samples, whereas reduced levels of *RGS16* were observed in 2/4 SS samples compared with normal CD4+ T cells (Fig. 3, B and C).

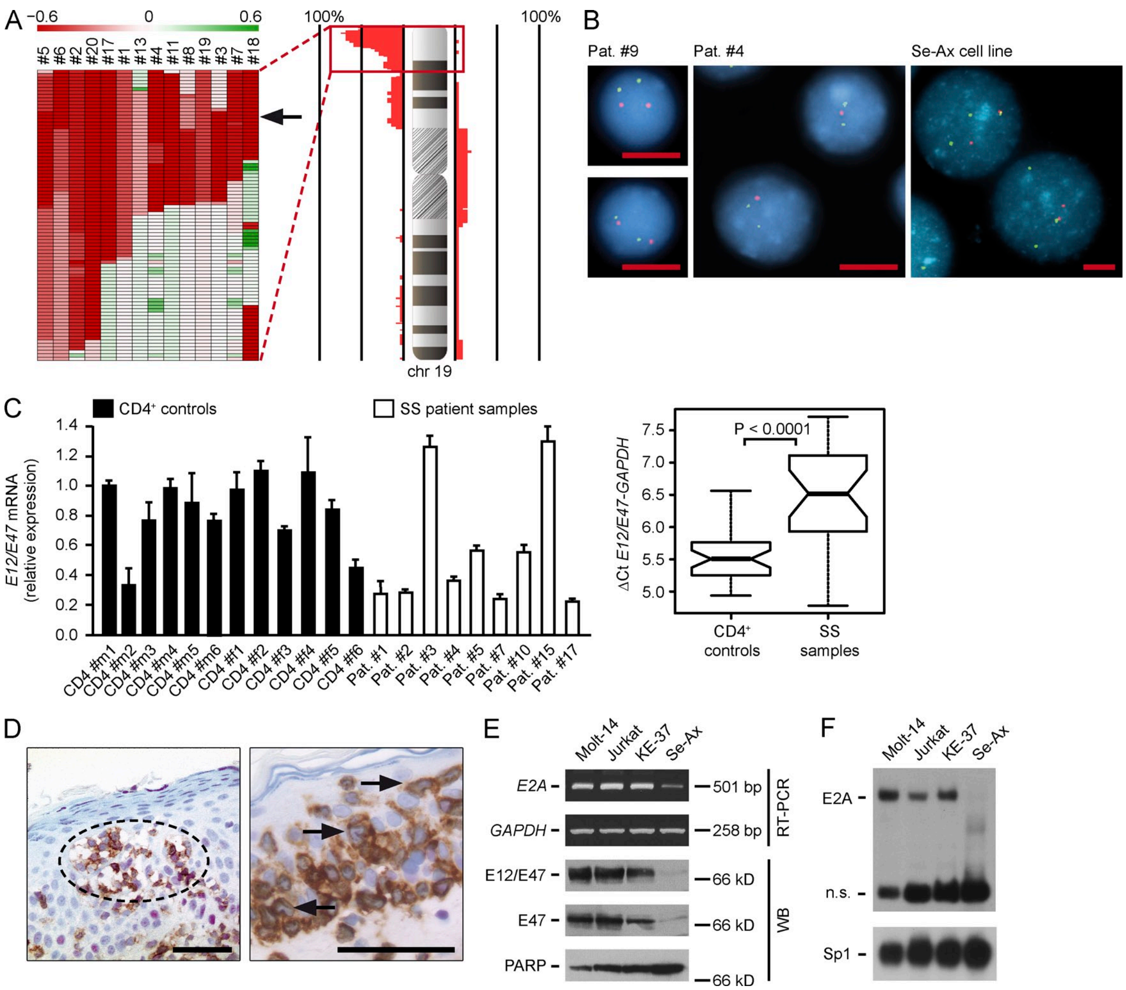

Figure 1. Loss of *E2A* is a common feature in SS tumor cells. (A) Array CGH results for chromosome 19 in tumor cells of 14 SS patients. The frequency of chromosomal gains and losses in percent of studied cases is shown to the right and to the left of the chromosome idiogram, respectively. The genomic interval ranging from chr19: 200000–8599999 (HG18) is enlarged in the adjacent heatmap to the left. The coloring of each box in this heatmap represents the average array CGH ratio based on a 100-kb window for those 14 cases harboring *E2A* deletions according to CGH results. Chromosomal deletions and gains are shown in red and green, respectively (maximal color saturation at a $\log_2$ ratio of 0.6/−0.6). The arrow indicates the genomic position of *E2A*. (B) Dual-color FISH analyses of purified tumor cells (patients #9 and #4) and the SS-derived cell line Se-Ax. Cells were hybridized with an *E2A* probe (red) and a control probe on 19qter (green). Pictures show representative examples of tumor cells without *E2A* deletion (Pat. #9: two red signals/two green signals) and cells with heterozygous deletion of the gene locus (Pat. #4, one red/two green; Se-Ax cells, two red/three green signals). Bars, 5 µm. (C) Quantification of *E2A* mRNA levels by real-time PCR in CD4+ T lymphocytes from healthy volunteers and purified leukemic SS cells from various patients, as indicated. (left) *E2A* mRNA expression in the various samples was analyzed relative to *GAPDH* by quantitative real-time PCR using primers recognizing both *E2A* splice variants, *E12* and *E47*. (right) Box plot presentation of the comparison of ΔCt values of *E2A* in CD4+ controls (six male [CD4 #m] and six female [CD4 #f] samples) and SS patient samples (Pat. #). Results are shown for one of two independent experiments performed. (D) Immunohistochemistry of SS skin biopsies. Shown is double staining of the T cell marker CD3 (brown) and E12/E47 (purple). Dashed circle designates accumulations of malignant lymphocytes in the epidermis, so called Pautrier's microabscesses. Arrows point to individual tumor cells with cerebriform nuclei. Bars, 50 µm. (E and F) E2A expression and DNA binding activity in various cell lines. (E, top) RT-PCR analysis of *E2A* mRNA expression in T cell–derived control cell lines Molt-14, Jurkat, and KE-37, as well as SS-derived Se-Ax cells. (bottom) Analysis of E2A protein expression in nuclear extracts of various cell lines by Western blotting (WB) using antibodies to both E2A splice variants E12 and E47 (E12/E47) or to E47. *GAPDH* and PARP were analyzed as controls. Results are shown for one of three independent experiments performed. (F) EMSA of E2A DNA-binding activity in the various cell lines, as indicated. Sp1 DNA binding was analyzed as a control. Positions of the specific protein–DNA complexes are indicated. n.s., nonspecific complex. Results are shown for one of three independent experiments performed.

Apart from their central role in B and T lymphocyte development, E2A proteins have been suggested to act as tumor suppressors (Bain et al., 1997; Yan et al., 1997). Although other genes located at 19p13.3 might also contribute to the pathogenesis of SS, our data identify the loss of *E2A* as a pathogenetically important defect of SS tumor cells and strongly support a role of *E2A* as a tumor suppressor in human lymphoid cells. Mechanistically, we provide evidence that E2A controls a whole set of genes known to promote tumorigenesis. Concomitant with an increased proliferation rate, most likely caused by an impaired G0/G1 cell cycle checkpoint, loss of *E2A* resulted in an up-regulation of *MYC* and *CDK6*. Both genes have been described as E2A target genes in lymphomas that emerge in *E2A*-deficient mice (Schwartz et al., 2006) and are known to be involved in lymphocyte proliferation, survival, and differentiation (Herold et al., 2009; Hu et al., 2009). Furthermore, aggressive T cell lymphomas in *E2A*-deficient mice are characterized by high-level *myc* expression (Bain et al., 1997). This suggests that up-regulation of the *MYC* oncogene is a common phenomenon after loss of E2A, most likely by loss of transcriptional repression. Speculations on the interconnection of MYC, E2A, and TP53 and their synergistic influence on lymphoma development are substantiated by the high number of cases with simultaneous DNA copy number changes affecting these genes in our SS samples, as well as in E2A-deficient lymphoma cells in mice, a fact that most likely reflects the selective advantage provided by the combination of these aberrations (Fig. S1 and Table S4; Bain et al., 1997). Up-regulation of CDK6 as a consequence of reduced E2A levels could represent another strategy of SS cells to provide a growth and survival advantage. Higher levels of CDK6 in SS cells might cooperate with an aberrant activation of the NOTCH signaling pathway, because CDK6 is necessary to exert the proliferative and anti-apoptotic function of NOTCH (Hu et al., 2009). NOTCH itself promotes T lymphomagenesis (Koch and Radtke, 2007) and is required for the survival of *E2A*-deficient lymphoma cells in mice (Reschly et al., 2006). In line with this concept, NOTCH activation has been reported in SS cells (Kamstrup et al., 2010). In addition, our data show that E2A controls negative regulators of the oncogenic

Table I. Loss of *E2A* in SS tumor cells

Patient no.	Loss of *E2A*		Purity of enriched tumor cells
	Array CGH analysis	FISH analysis (number of cells with deletion/number of analyzed cells)	
			%
1	yes[c]	yes (149/200)[e]	96.7
2	yes[c]	n.d	–
3	yes[c]	yes (198/200)[e]	99.1
4[a]	yes[c]	yes (167/200)[e]	93.2
5	yes[e]	yes (90/200)[e]	97.9
6	yes[d]	n.d.	–
7[a]	yes[c]	no (14/200)[e]	99.2[f]
8	yes[e]	n.d.	–
9	no[c]	no (3/200)[e]	97.4
10	no[c]	no (4/200)[e]	96.9
11[a]	yes[e]	no (12/200)[d]	n.d.
12	no[c]	n.d.	–
13	yes[c]	yes (126/200)[e]	98.4[f]
14	no[c]	n.d.	–
15[a]	no[b,c]	yes (106/200)[d]	n.d.
16[a]	no[e]	yes (loss 28/200, gain 46/200)[e]	97.2
17	yes[e]	yes (50/200)[e]	98.4
18	yes[c]	n.d.	–
19	yes[e]	n.d.	–
20	yes[e]	n.d.	–
Se-Ax cell line	yes	yes (190/200)	

n.d.: not determined
[a]CGH and FISH analyses were performed with samples from different time points (see Table S1).
[b]hypotriploid cells, gain of chromosome 19 except 19p13.2-13.3.
[c]Analysis of PBMC cells.
[d]Analysis of CD4-sorted cells.
[e]Analysis of Vβ-sorted cells.
[f]Purity was determined with CD4 antibody only.

Ras signaling pathway (*RASSF4*, *RASA4*, and *DAB2IP*). Although altered expression of each of these genes alone might result in Ras activation (Eckfeld et al., 2004; Lockyer et al., 2001; Min et al., 2010), activation of the Ras signaling pathway has still to be proven formally in SS cells. Therefore, the therapeutic potential of Ras inhibition in lymphomas with reduced E2A activity has to be investigated in future studies.

By FISH analysis, no homozygous deletion of *E2A* was observed. Direct sequencing of the coding regions of all *E2A* exons in leukemic SS cells from 13 patients did not reveal deleterious mutations or deletions (Table S7). Furthermore, the investigated *E2A* promoter regions in enriched SS cells compared with normal CD4+ T cells did not show altered methylation patterns Fig. S4. These data suggest on the one hand that the reduction of E2A expression after monoallelic *E2A* deletion might be sufficient for lymphoma progression, and on the other hand that selective pressure exists to retain one *E2A* copy to ensure a certain level of E protein activity, which is probably necessary for cellular survival at some time point during lymphomagenesis. Lowering the E2A dosage might facilitate the posttranslational degradation of E2A by NOTCH1 (Nie et al., 2003), which is aberrantly activated in SS cells (Kamstrup et al., 2010). Such a model, i.e., that lowering of wild-type E2A expression contributes to human lymphomagenesis, is supported by the finding of aberrant up-regulation of E2A antagonists like inhibitory HLH proteins (O'Neil et al., 2004; Lietz et al., 2007; Mathas et al., 2006, 2009) or the disruption of one *E2A* allele and maintenance of one wild-type allele as a result of translocations involving the *E2A* locus (Aspland et al., 2001) in human lymphoma cells. That even a subtle dosage reduction of a putative tumor suppressor is sufficient for tumor formation has recently been formally shown for, e.g., PTEN (Alimonti et al., 2010).

Together, our data highlight the genomic loss of 19p13.3 including the *E2A* locus as a pathogenetically important defect of human T cell–derived SS lymphoma cells. Our results provide insights into how E2A acts as a tumor suppressor in human lymphoid cells and might help to develop new treatment strategies for human lymphomas with lost or reduced E2A activity.

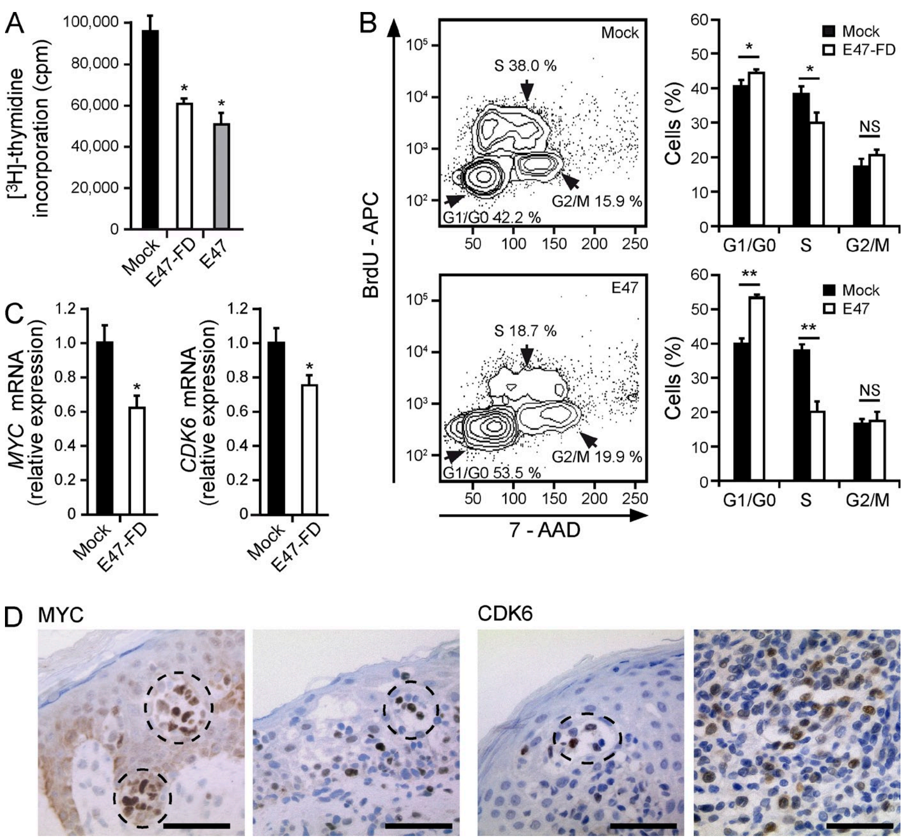

Figure 2. E2A-dependent proliferation and expression of MYC and CDK6 in SS cells. (A) Reconstitution of E2A expression in SS-derived Se-Ax cells. Se-Ax cells were transfected with Mock plasmid (control) or plasmids encoding Myc-tagged E47 (E47) or E47-FD, as indicated, along with pEGFP. EGFP+ cells were purified 48 h after transfection, pulsed with 1 µCi [3H]thymidine per well for another 20 h, and then [3H]thymidine incorporation was determined. Error bars denote standard deviation. Results are shown for one of three independent experiments performed. *, $P < 0.001$. (B) Proliferation and cell cycle analyses of Se-Ax cells after E2A reconstitution. Se-Ax cells were transfected as described in A. 48 h after transfection, cells were pulsed for 30 min with BrdU. Thereafter, transfected cells were gated based on their EGFP expression, and BrdU incorporation and 7-AAD staining was measured by flow cytometry in GFP+ cells. Left, representative examples for detection of BrdU incorporation and 7-AAD staining by flow cytometry in Mock- (top) or E47- (bottom) transfected Se-Ax cells. Positions and percentages of cells in cell cycle phases G0/G1, S, and G2/M are indicated. Right, summary of cell cycle analyses of Mock- vs. E47-FD– (top) and E47- (bottom) transfected Se-Ax cells. The fraction of cells in the respective cell cycle phases is indicated in percent. Error bars denote standard deviations. Results are shown for one of three independent experiments performed. *, $P < 0.05$; **, $P < 0.005$; NS, not significant. (C) Se-Ax cells were transfected with E47-FD and purified as described in A. Expression of *MYC* and *CDK6* mRNA was assessed by quantitative PCR. Error bars denote 95% confidence intervals. Results are shown for one of three independent experiments performed. *, $P < 0.001$. (D) Representative MYC and CDK6 immunohistochemistry of each two SS skin biopsies. MYC and CDK6 stainings are in brown. Dashed circles designate Pautrier's microabscesses. CDK6, right, CDK6 expression in cells with frequent cerebriform nuclei within a dermal infiltrate from a patient with SS. Bars, 50 µm.

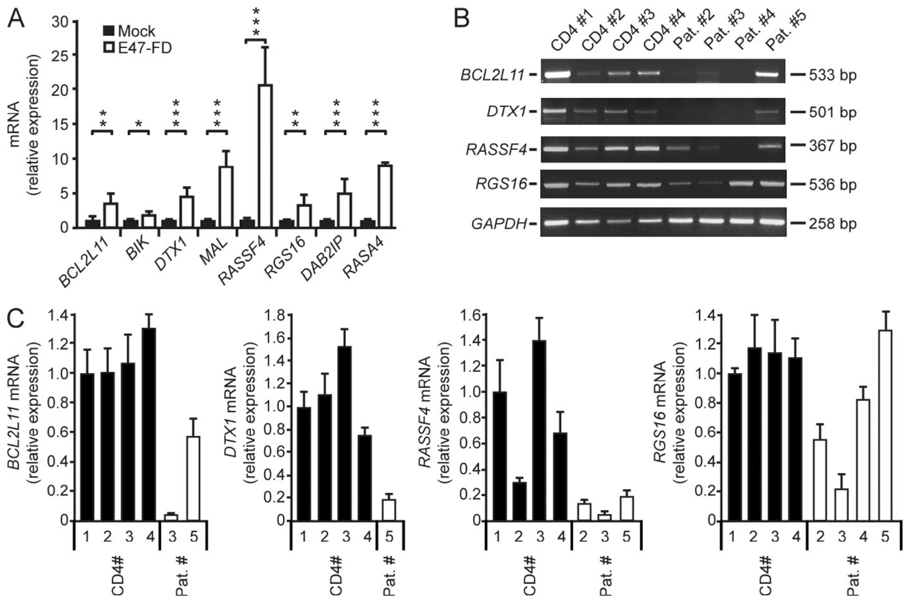

Figure 3. E2A-regulated genes in SS tumor cells. (A) Se-Ax cells were transfected with Mock plasmids (control) or plasmids encoding E47-FD, along with pEGFP. 48 h after transfection, EGFP⁺ cells were enriched. Expression of various genes, as indicated, was assessed by quantitative PCR. Error bars denote 95% confidence intervals. Results are shown for one of four independent experiments performed. *, $P < 0.5$; **, $P < 0.01$; ***, $P < 0.001$. (B and C) mRNA expression of various genes in purified CD4⁺ T cells from healthy donors (CD4 #1 to CD4 #4) compared with enriched tumor cells derived from four SS patients (Pat. #2, #3, #4, #5; numbers refer to the same patients listed in Table I). If mRNA expression was detectable in SS samples by semiquantitative PCR (B), mRNA expression was quantified by real-time PCR in the respective samples (C). Error bars denote 95% confidence intervals. Results are shown for one of two independent experiments performed.

MATERIALS AND METHODS

Patient samples. 20 clinically well-characterized patients with SS were included in our study. Diagnoses were established according to the World Health Organization-European Organization for Research and Treatment of Cancer classification for cutaneous lymphomas (Willemze et al., 2005). Detailed clinical information on all patients and blood samples are summarized in Table S1. The use of human material was approved by the Local Ethics Committee of the Charité-Universitätsmedizin Berlin and performed in accordance with the Declaration of Helsinki.

Clonality analysis and sequencing of tumor cell–specific TCRβ rearrangements. PBMC samples were analyzed for the presence of a clonally expanded tumor cell population by TCRβ-rearrangement PCR analysis using primers and protocols developed within the BIOMED-2 BMH4-CT98-3936 Concerted Action initiative (van Dongen et al., 2003). Only samples that showed almost single clonal product peaks in the fluorescent fragment analysis (FFA) were directly used for subsequent CGH analysis. To identify the Vβ chain expressed by the respective tumor cells, amplification products were purified and complete TCRβ rearrangements were sequenced using the BigDye Terminator V1.1 cycle sequencing kit (Applied Biosystems) and subsequent analysis by high resolution electrophoresis on an ABI PRISM 310 Genetic Analyzer. Identification of the involved V, D, and J segments was done by submitting the received TCRβ sequence to the International Immunogenetics Information System V-QUEST tool (http://imgt.cines.fr/IMGT_vquest/share/textes/; Brochet et al., 2008; Lefranc et al., 2009). Results for each patient are presented in Table S3.

Enrichment of primary SS tumor cells from PBMCs. PBMCs were isolated from whole blood or leukapheresis samples by density gradient centrifugation using Ficoll-Paque-Plus (GE Healthcare). For enrichment of tumor cells, PBMCs were incubated for 30 min with the respective fluorochrome-conjugated Vβ antibody (Beckman Coulter; see Table S3 for details) at a concentration of 5–20 µl/10^6 cells in 100 µl of MACS buffer, followed by incubation with anti-fluorochrome MicroBeads (Miltenyi Biotec). Cells were magnetically separated by use of LS columns (Miltenyi Biotec) according to the manufacturer's recommendations. Where indicated, tumor cells were enriched after incubation with anti-CD4 microbeads (Miltenyi Biotec). The purity of enriched cells was determined by flow cytometry.

Flow cytometric analysis of tumor cell samples. PBMCs and enriched tumor cells were analyzed on a FACSCalibur flow cytometer (BD) using CellQuest Pro software (BD) and WinMDI version 2.9 (The Scripps Research Institute). Antibodies directed against CD3, CD4, and CD8 were purchased from BD. All Vβ−chain specific antibodies were from Beckman Coulter (see Table S3 for details).

Cell lines, culture conditions, proliferation, and cell cycle analysis. The human SS-derived cell line Se-Ax (Kaltoft et al., 1987); the T cell acute lymphoblastic leukemia (T-ALL) cell lines Molt-14, Jurkat, and KE-37; and H9 cells were cultured as previously described (Mathas et al., 2009), apart from adding 100 U/ml recombinant human IL-2 (Sigma-Aldrich) to Se-Ax cell culture medium. Se-Ax cells were electroporated in OPTIMEM I (Invitrogen) using a Gene-Pulser II (Bio-Rad Laboratories) with 500 µF and 0.24 kV. Transfection efficiency was determined by pEGFP-N3 (Takara Bio Inc.) co-transfection and subsequent flow cytometry. Cells were transfected with 30 µg myc-tagged E47 or E47-FD expression constructs (Sigvardsson et al., 1997; Lietz et al., 2007) or 30 µg control plasmid pcDNA3.1 (Invitrogen), along with 10 µg of pEGFP-N3. 48–72 h after transfection, EGFP⁺ cells were enriched by FACS sorting, and sorted cells were used for proliferation assays as well as RNA and protein preparation. Proliferation of cells was determined by measurement of DNA synthesis after [^{3}H]thymidine incorporation using standard protocols. Parallel measurement of BrdU incorporation for determination of proliferation and of 7-AAD staining for determination of cell cycle position was performed by use of the APC BrdU Flow kit (BD). In brief, 48 h after transfection, cells were pulsed for 30 min with BrdU, and BrdU incorporation and 7-AAD staining in gated EGFP⁺ cells was determined by flow cytometry.

Array CGH. Initial array CGH analysis was done by means of a submegabase resolution BAC array, as described previously (Erdogan et al., 2006). DNA copy number changes were defined by circular binary segmentation (Olshen et al., 2004) in combination with a $\log_2$ threshold of 0.2/−0.2. Aberrations encompassing chromosome arm 19p were further verified and fine-mapped by hybridizations onto a 400k whole genome (Agilent; Gene Expression Omnibus [GEO] accession no. GPL9777) and a customized 60k chromosome 19p oligonucleotide array (Agilent; GEO accession no. GPL10304), respectively, following the manufacturer's recommendations (Table S8). The customized array comprised 52,828 oligonucleotides evenly covering chromosomal region chr19: 1–28,500,000 (NCBI36; HG18). Array CGH data discussed in this work are available (Barrett and Edgar, 2006) under GEO accession no. GSE19000.

FISH analysis of *E2A*. FISH analysis was performed on enriched tumor cells using the specific DNA-probes spanning the *E2A* gene (RP11-690N6) and control probes for 19qter (D19S989; Kreatech) to judge the copy number of chromosome 19. Hybridization, detection, dual color image acquisition, and image analysis were performed as previously described (Schröck and Padilla-Nash, 2000).

RNA preparation, semiquantitative, and real-time PCR analyses. Total RNA was prepared using the RNeasy kit (QIAGEN). First strand cDNA-synthesis was performed by use of the first-strand cDNA synthesis kit (AMV; Roche) adding oligo-p(dT)15 primer according to the manufacturer's recommendation. For semiquantitative PCR analyses primers were as follows: *GAPDH*, sense (s) 5′-ATGCTGGCGCTGAGTAC-3′ and antisense (as) 5′-TGAGTCCTTCCACGATAC-3′; *E2A*, s 5′-CACCCTCCCTGACCTGTCT-3′ and as 5′-GGAGCTGAAAGCACCATCTG-3′; *RGS16*, s 5′-TGGAGAGAGTCGTTCGACCTG-3′ and as 5′-TGTCCTCTTGCACTTGCTTTGC-3′; *RASSF4*, s 5′-GGTGGGGATGACTTTCAATG-3′ and as 5′-GTGGCTTCCAAGCTATGCTC-3′; *BCL2L11* s 5′-GGGTGACTGGAGAGCTCATT-3′ and as 5′-AAAGCACAGGAAGTTGCACA-3′; *DTX1*, s 5′-CTGGTCACAGCATCAGGCTA-3′ and as 5′-GGTCTTGTGGTGGATCTCGT-3′. Real-time PCR analyses were performed using Power SYBR Green Mastermix and the ABI StepOnePlus real-time PCR system (Applied Biosystems). Three technical replicates were performed for each reaction and specificity of PCR products was confirmed by melting curve analysis and subsequent agarose gel electrophoresis. Relative expression values were determined using the $2^{-\Delta\Delta Ct}$ method. Calculations were done with the StepOnePlus software, taking into account the determined primer efficiency of each primer set used. Primers used for real-time PCR analyses were as follows: *myc*, s 5′-TCAAGAGGTGCCACGTCTCC-3′ and as 5′-TCTTGGCAGCAGGATAGTCCTT-3′; *CDK6*, s 5′-GGCTGTGTGAACCAGCCCAAG-3′ and as 5′-TGGCCAGGCCTAGACAGGCA-3′; *DTX1*, s 5′-TCAGGCTACGAGGGCGTGCT-3′ and as 5′-CCACGAGGCACAGCAGGTGG-3′; *BIK*, s 5′-AGCTCCTGGAACCCCCGACC-3′ and as 5′-CGCAGGGCCAATGCGTCACT-3′; *MAL*, s 5′-GGTGGGAAGTGGCGACCGTG-3′ and as 5′-ACAAGATGGGGCGCTCGGGA-3′; *RASSF4*, s 5′-TTGGGCGTGGAAGTCCCCCA-3′ and as 5′-AGGCGCTGCAGCATCGTCAG-3′; *BCL2L11*, s 5′-TGCCAGCCCTGGCCCTTTTG-3′ and as 5′-GGCCTGGCAAGGAGGACTTGG-3′; *RGS16*, s 5′-TCAGCCGCCTCTGCCACTCT-3′ and as 5′-CGGCTGGCTTCCTCACTGCC-3′; *RASA4*, s 5′-TTTGGCGGCTCGCACGTCAT-3′ and as 5′-CACCTTCCGCAGCGCAGACA-3′; *DAB2IP*, s 5′-CTGTGTGCAGCCCTCGAGCC-3′ and as 5′-GAGGTGCTCGTTGTCCCCGC-3′; *TBP*, s 5′-CAGGAGCCAAGAGTGAAGAACA-3′ and as 5′-AGCTGGAAAACCCAACTTCTGT-3′; *GAPDH*, s 5′-CTCTGCTCCTCCTGTTCGAC-3′ and as 5′-TTAAAAGCAGCCCTGGTGAC-3′; TaqMan Gene Expression Assays Hs01012686_m1 (*E47*), Hs0102692_g1 (*E12/E47*), and Hs03929097_g1 (*GAPDH*). For statistical analyses, independent Student's *t* tests were used. All PCR products were verified by sequencing.

Direct sequencing of *E2A* coding regions. All 18 coding exons of *E2A* (E12 and E47) were amplified from 10–20 ng of genomic DNA isolated from enriched tumor cells using AccuPrime GC-Rich Polymerase (Invitrogen) according to the manufacturer's recommendations. PCR products were directly sequenced by using the BigDye Terminator V1.1 cycle sequencing kit (Applied Biosystems) and subsequent analysis on an ABI PRISM 310 Genetic Analyzer. Primer sequences for amplification and sequencing were as follows: Exon 1, s 5′-CCTCCCTGTTTCTCCCTGTC-3′ and as 5′-GAAAACCTTCCCGTGAACTG-3′; Exon 2, s 5′-TGTAGGGTTTGGTTTGCCAC-3′ and as 5′-CACTGTCTTCAACAGACCCTTG-3′; Exon 3, s 5′-AGGTTTGCCCCTGAGATGAT-3′ and 3 as 5′-CAGGACTCAAACCCATGTCC-3′; Exon 4, s 5′-GGACATGGGTTTGAGTCCTG-3′ and as 5′-GTGAACGCTGGGGACTTG-3′; Exon 5, s 5′-CCCTCAGGATGTTCCTTGGG-3′ and as 5′-GAGAGGGTGGGTGACAGATTTG-3′; Exon 6, s 5′-AACAGCCTGGGGTCTGGATG-3′ and as 5′-CCTACCTCCCTTTGCAGGCT-3′; Exon 7, s 5′-GCAGGGGTTGTTCTCATGGC-3′ and as 5′-AAGCTTCGCCAGGACACAGG-3′; Exon 8, s 5′-GAAACGGGGTGGTAGATGTG-3′ and as 5′-GAGGGGAGCTGGTAAGGTG-3′; Exon 9, s 5′-CTATCCCGCCCCCTTCTAC-3′ and as 5′-GTTCACCTCTGCTCCATGC-3′; Exon 10, s 5′-GCACGAGCGTATGGTAGGAC-3′ and as 5′-CTCTCAGGGCCAGCAGAC-3′; Exon 11+12, s 5′-CTGTGCAGGACGGCAGAAC-3′ and as 5′-CCGCAAAGCCTTCACAGA-3′; Exon 13, s 5′-ATCAGGCCATGCTCACACCC-3′ and as 5′-TCTGTCCTGCAAATTCTGTCGG-3′; Exon 14, s 5′-CATGCGGAAGGGACATGA-3′ and as 5′-GGTGGCTGCCTCCAACCT-3′; Exon 15, s 5′-GCTGGCCTCAGGTTTCAC-3′ and as 5′-ACCCTGACCCCCACCACTA-3′; Exon 16a, s 5′-CCAAGACCTGGTTTTTCCAG-3′ and as 5′-GAGGGAGACAGTGAGGTTGG-3′; Exon 16b, s 5′-ACCCACACTGGGAGGCCGT-3′ and as 5′-CAGTCATGGCAATGCGGTCA-3′; Exon 17, s 5′-TACCCTCTCCACAACCCAGC-3′ and as 5′-AGCATCTGCACCTGGGTGTG-3′; Exon 18, s 5′-ACATCTTTCTCCTCCCTGGG-3′ and as 5′-GTGTGGATGTGGATGAAGCC-3′.

Bisulfite pyrosequencing. Bisulfite pyrosequencing of two amplicons located in the *E2A* promoter region was performed according to Lamprecht et al., 2010 with few modifications. In brief, genomic DNA was bisulfite converted using the EpiTect Bisulfite Conversion kit (QIAGEN). In a post-PCR amplification, locus-specific primers were used with one primer biotinylated at the 5′ end (PCR and sequencing primer sequences and analyzed region are shown in the following paragraph). For *E2A* amplification reactions, PyroMark PCR kit (QIAGEN) was used according to standard protocols. After initial denaturation (95°C for 15 min), PCR consisted of 45 cycles of 94°C for 30 s, annealing temperature for 30 s, and 72°C for 30 s, followed by a final synthesis at 72°C for 10 min. Pyrosequencing was performed using the Pyrosequencer ID and the DNA methylation analysis software Pyro Q-CpG 1.0.9 (Biotage), which was also used to evaluate the ratio T:C (mC:C) at the CpG sites analyzed. All assays were optimized and validated using commercially available completely methylated DNA (Millipore) and pooled DNA isolated from peripheral blood of 10 healthy male and female controls, respectively.

Primer sequences and conditions used for bisulfite-pyrosequencing were as follows: *E2A*_promA, s 5′-TTAGTTTATGGAGGGTAGGTA-3′ (5′ modification, biotin) and as 5′-AAACCCCAACAATATTCA-3′ (annealing temperature, 55°C; amplicon length, 126 bp; analyzed region [ucsc, HG18], chr19:1,601,941-1,602,066); *E2A*_promA_seq, 5′-CCCTAAATTACTTTACTAT-3′; *E2A*_promB, s 5′-TAAGGGGGAAATTGAGGT-3′ and as 5′-CCCTAATACTAAACCCTACATACAA-3′ (5′ modification, biotin; annealing temperature, 55°C; amplicon length, 139 bp; analyzed region [ucsc, HG18], chr19:1,596,870-1,597,008); *E2A*_promB_seq, 5′-ATTGAGGTTTTGGAG-3′.

Electrophoretic mobility shift assay (EMSA) and immunoblotting. Preparation of whole-cell and nuclear extracts, as well as EMSA, was performed as previously described (Mathas et al., 2006). The following double-stranded oligonucleotides were used for EMSA: E2A (μE5) sense 5′-AGCTCCAGAACACCTGCAGCAG-3′ and E2A (μE5) antisense, 5′-AGCTCTGCTGCAGGTGTTCTGG-3′; Sp1 sense, 5′-AGCTATTCGATCGGGGCGGGGCGAGC-3′ and Sp1 antisense, 5′-AGCTGCTCGCCCCGCCCCGATCGAAT-3′. After annealing, oligonucleotides were end-labeled with [α-^{32}P]dCTP using Klenow fragment. Positions of protein–DNA complexes were visualized by autoradiography. For supershift analyses, mouse monoclonal antibody to E12/E47 (clone G98-271; BD) was used. For immunoblot analyses, the following primary antibodies were used: mouse monoclonal antibody to E12/E47 (clone G98-271; BD), mouse monoclonal antibody to E47 (clone G127-32; BD), goat polyclonal antibody to PARP-1 (sc-1561; Santa Cruz Biotechnology, Inc.), and mouse monoclonal antibody to β-actin (A5316; Sigma-Aldrich). Filters were incubated with horseradish peroxidase–conjugated secondary antibodies. Bands were visualized with the enhanced chemiluminescence system (GE Healthcare).

Immunohistochemistry. Immunohistochemistry was performed on 4-μm sections obtained from formalin-fixed and paraffin-embedded material, and done according to Mathas et al., 2009. The primary antibodies used for evaluation of various proteins were monoclonal antibody to E12/E47 (clone G98-271; BD), CDK6 (clone DCS-83; Progen Biotechnik), myc (clone Y69; Epitomics), and CD3 (clone LN10; Novocastra Laboratories).

Gene expression analysis. One-color microarray-based gene expression analysis was performed following the Quick Amp Labeling protocol from Agilent (G4140-90040v5.7; Agilent). In brief, 500 ng of total RNA was reverse transcribed, and the cDNAs were used as a template for cRNA synthesis and Cy3 labeling by in vitro transcription. Hybridization was performed on whole human genome 4 × 44k microarrays (G4112F; Agilent; GEO accession no. GPL6480). After washing, slides were scanned using an Agilent DNA Microarray Scanner G2565BA with the following settings: scan region, 61 × 21.6 mm; scan resolution, 5 μm; extended dynamic range, selected; TIFF, 16 bit; dye channel, green (with Green PMT XDR Hi 100% and Green PMT XDR Lo 10%). The resulting TIFF images were processed with Agilent Feature Extraction Software v10.5.1.1 using the GE1_105_Dec08 protocol. Gene expression data discussed in this work (Barrett and Edgar, 2006) are available under GEO accession no. GSE21730.

Statistical analyses. All statistical analyses were done in R v2.9.1 (http://www.r-project.org/). Independent, one-tailed Student's *t* test was used to analyze data from real-time PCR experiments. For analyses of proliferation assays, one-way analysis of variance was done before applying Tukey's Honestly Significant Difference test with 95% family-wise confidence level. Two-sided Welch's *t* test was applied to determine significance of cell cycle phase differences between Mock- and E47-FD– or E47-transfected cells, respectively.

Online supplemental material. In Fig. S1, the complete copy number changes detected by array CGH analysis of all analyzed patients are depicted. Fig. S2 shows a clonality analysis of a leukemic SS patient before and after tumor cell enrichment. Fig. S3 shows *E47* mRNA expression levels in SS patient samples. Fig. S4 shows methylation of two regions within the promoter region of *E2A* in SS patient samples compared with purified CD4$^+$ T lymphocytes from healthy volunteers. Table S1 shows detailed information on SS patient samples. Table S2 shows the exact positions of the 19p13.3 deletion in every individual patient. Table S3 presents the TCRβ rearrangements of the clonal tumor cell population and the antibodies used for detecting/enrichment of the tumor cells. Table S4 shows chromosomal copy number alterations of *TP53* and *myc* in our SS samples. Table S5 gives a complete list of E2A-regulated genes in Se-Ax cells. Table S6 shows the overlap between our dataset and datasets derived from murine *E2A*-deficient cell types. Table S7 presents all detected sequence alterations within the *E2A* coding region. Table S8 gives an overview of the used CGH array platforms. Online supplemental material is available at http://www.jem.org/cgi/content/full/jem.20101785/DC1.

Funding was provided in part by Framework VII EU (European Union/BMBF-0315207A) grant, the Deutsche Forschungsgemeinschaft (TRR54), the Berliner Krebsgesellschaft, and the Max Planck Innovation Fonds. We thank Linda El-Ahmad, Franziska Hummel, Simone Kressmann, Katrin Tebel, and Arleta Frensel for excellent technical assistance, and Peter Rahn for cell sorting.

A. Steininger and M. Möbs designed and performed experiments and contributed to writing of the paper. I. Anagnostopoulos, M. Hummel, and H. Stein provided material and performed and interpreted immunohistochemistry analyses. K. Köchert, B. Lamprecht, and S. Kreher performed experiments and interpreted data. M. Beyer and C.D. Klemke provided material. E. Schrock designed and interpreted FISH analyses. J. Richter designed and interpreted bisulfite pyrosequencing analyses. B. Dörken, W. Sterry, E. Schrock, and M. Janz interpreted data and contributed to writing of the manuscript. R. Ullmann, S. Mathas, and C. Assaf designed the study, interpreted data, and wrote the manuscript.

The authors declare no competing financial interests.

Submitted: 27 August 2010
Accepted: 17 June 2011

REFERENCES

Alimonti, A., A. Carracedo, J.G. Clohessy, L.C. Trotman, C. Nardella, A. Egia, L. Salmena, K. Sampieri, W.J. Haveman, E. Brogi, et al. 2010. Subtle variations in Pten dose determine cancer susceptibility. *Nat. Genet*. 42:454–458. doi:10.1038/ng.556

Aspland, S.E., H.H. Bendall, and C. Murre. 2001. The role of E2A-PBX1 in leukemogenesis. *Oncogene*. 20:5708–5717. doi:10.1038/sj.onc.1204592

Bain, G., I. Engel, E.C. Robanus Maandag, H.P. te Riele, J.R. Voland, L.L. Sharp, J. Chun, B. Huey, D. Pinkel, and C. Murre. 1997. E2A deficiency leads to abnormalities in alphabeta T-cell development and to rapid development of T-cell lymphomas. *Mol. Cell. Biol*. 17:4782–4791.

Barrett, T., and R. Edgar. 2006. Gene expression omnibus: microarray data storage, submission, retrieval, and analysis. *Methods Enzymol*. 411:352–369. doi:10.1016/S0076-6879(06)11019-8

Brochet, X., M.P. Lefranc, and V. Giudicelli. 2008. IMGT/V-QUEST: the highly customized and integrated system for IG and TR standardized V-J and V-D-J sequence analysis. *Nucleic Acids Res*. 36(Web Server issue):W503-W508. doi:10.1093/nar/gkn316

Eckfeld, K., L. Hesson, M.D. Vos, I. Bieche, F. Latif, and G.J. Clark. 2004. RASSF4/AD037 is a potential ras effector/tumor suppressor of the RASSF family. *Cancer Res*. 64:8688–8693. doi:10.1158/0008-5472.CAN-04-2065

Eischen, C.M., J.D. Weber, M.F. Roussel, C.J. Sherr, and J.L. Cleveland. 1999. Disruption of the ARF-Mdm2-p53 tumor suppressor pathway in Myc-induced lymphomagenesis. *Genes Dev*. 13:2658–2669. doi:10.1101/gad.13.20.2658

Erdogan, F., W. Chen, M. Kirchhoff, V.M. Kalscheuer, C. Hultschig, I. Müller, R. Schulz, C. Menzel, T. Bryndorf, H.H. Ropers, and R. Ullmann. 2006. Impact of low copy repeats on the generation of balanced and unbalanced chromosomal aberrations in mental retardation. *Cytogenet. Genome Res*. 115:247–253. doi:10.1159/000095921

Herold, S., B. Herkert, and M. Eilers. 2009. Facilitating replication under stress: an oncogenic function of MYC? *Nat. Rev. Cancer*. 9:441–444. doi:10.1038/nrc2640

Hu, M.G., A. Deshpande, M. Enos, D. Mao, E.A. Hinds, G.F. Hu, R. Chang, Z. Guo, M. Dose, C. Mao, et al. 2009. A requirement for cyclin-dependent kinase 6 in thymocyte development and tumorigenesis. *Cancer Res*. 69:810–818. doi:10.1158/0008-5472.CAN-08-2473

Ikawa, T., H. Kawamoto, A.W. Goldrath, and C. Murre. 2006. E proteins and Notch signaling cooperate to promote T cell lineage specification and commitment. *J. Exp. Med*. 203:1329–1342. doi:10.1084/jem.20060268

Kaltoft, K., S. Bisballe, H.F. Rasmussen, K. Thestrup-Pedersen, K. Thomsen, and W. Sterry. 1987. A continuous T-cell line from a patient with Sézary syndrome. *Arch. Dermatol. Res*. 279:293–298. doi:10.1007/BF00431220

Kamstrup, M.R., L.M. Gjerdrum, E. Biskup, B.T. Lauenborg, E. Ralfkiaer, A. Woetmann, N. Ødum, and R. Gniadecki. 2010. Notch1 as a potential therapeutic target in cutaneous T-cell lymphoma. *Blood*. 116:2504–2512. doi:10.1182/blood-2009-12-260216

Kari, L., A. Loboda, M. Nebozhyn, A.H. Rook, E.C. Vonderheid, C. Nichols, D. Virok, C. Chang, W.H. Horng, J. Johnston, et al. 2003. Classification and prediction of survival in patients with the leukemic phase of cutaneous T cell lymphoma. *J. Exp. Med*. 197:1477–1488. doi:10.1084/jem.20021726

Kee, B.L. 2009. E and ID proteins branch out. *Nat. Rev. Immunol*. 9:175–184. doi:10.1038/nri2507

Koch, U., and F. Radtke. 2007. Notch and cancer: a double-edged sword. *Cell. Mol. Life Sci*. 64:2746–2762. doi:10.1007/s00018-007-7164-1

Lamprecht, B., K. Walter, S. Kreher, R. Kumar, M. Hummel, D. Lenze, K. Köchert, M.A. Bouhlel, J. Richter, E. Soler, et al. 2010. Derepression of an endogenous long terminal repeat activates the CSF1R proto-oncogene in human lymphoma. *Nat. Med*. 16:571–579: 1p: 579. doi:10.1038/nm.2129

Lefranc, M.P., V. Giudicelli, C. Ginestoux, J. Jabado-Michaloud, G. Folch, F. Bellahcene, Y. Wu, E. Gemrot, X. Brochet, J. Lane, et al. 2009. IMGT, the international ImMunoGeneTics information system. *Nucleic Acids Res*. 37(Database issue):D1006–D1012. doi:10.1093/nar/gkn838

Lietz, A., M. Janz, M. Sigvardsson, F. Jundt, B. Dörken, and S. Mathas. 2007. Loss of bHLH transcription factor E2A activity in primary effusion lymphoma confers resistance to apoptosis. *Br. J. Haematol*. 137:342–348. doi:10.1111/j.1365-2141.2007.06583.x

Lockyer, P.J., S. Kupzig, and P.J. Cullen. 2001. CAPRI regulates Ca(2+)-dependent inactivation of the Ras-MAPK pathway. *Curr. Biol*. 11:981–986. doi:10.1016/S0960-9822(01)00261-5

Mathas, S., M. Janz, F. Hummel, M. Hummel, B. Wollert-Wulf, S. Lusatis, I. Anagnostopoulos, A. Lietz, M. Sigvardsson, F. Jundt, et al. 2006. Intrinsic inhibition of transcription factor E2A by HLH proteins ABF-1 and Id2 mediates reprogramming of neoplastic B cells in Hodgkin lymphoma. *Nat. Immunol*. 7:207–215. doi:10.1038/ni1285

Mathas, S., S. Kreher, K.J. Meaburn, K. Jöhrens, B. Lamprecht, C. Assaf, W. Sterry, M.E. Kadin, M. Daibata, S. Joos, et al. 2009. Gene deregulation and spatial genome reorganization near breakpoints prior to formation of translocations in anaplastic large cell lymphoma. *Proc. Natl. Acad. Sci. USA*. 106:5831–5836. doi:10.1073/pnas.0900912106

Mellentin, J.D., C. Murre, T.A. Donlon, P.S. McCaw, S.D. Smith, A.J. Carroll, M.E. McDonald, D. Baltimore, and M.L. Cleary. 1989. The gene for enhancer binding proteins E12/E47 lies at the t(1;19) breakpoint in acute leukemias. *Science*. 246:379–382. doi:10.1126/science.2799390

Min, J., A. Zaslavsky, G. Fedele, S.K. McLaughlin, E.E. Reczek, T. De Raedt, I. Guney, D.E. Strochlic, L.E. Macconaill, R. Beroukhim, et al. 2010. An oncogene-tumor suppressor cascade drives metastatic prostate cancer by coordinately activating Ras and nuclear factor-kappaB. *Nat. Med*. 16:286–294. doi:10.1038/nm.2100

Morrow, M.A., E.W. Mayer, C.A. Perez, M. Adlam, and G. Siu. 1999. Overexpression of the Helix-Loop-Helix protein Id2 blocks T cell development at multiple stages. *Mol. Immunol*. 36:491–503. doi:10.1016/S0161-5890(99)00071-1

Murre, C. 2005. Helix-loop-helix proteins and lymphocyte development. *Nat. Immunol*. 6:1079–1086. doi:10.1038/ni1260

Murre, C., P.S. McCaw, and D. Baltimore. 1989. A new DNA binding and dimerization motif in immunoglobulin enhancer binding, daughterless, MyoD, and myc proteins. *Cell*. 56:777–783. doi:10.1016/0092-8674(89)90682-X

Nie, L., M. Xu, A. Vladimirova, and X.H. Sun. 2003. Notch-induced E2A ubiquitination and degradation are controlled by MAP kinase activities. *EMBO J*. 22:5780–5792. doi:10.1093/emboj/cdg567

O'Neil, J., J. Shank, N. Cusson, C. Murre, and M. Kelliher. 2004. TAL1/SCL induces leukemia by inhibiting the transcriptional activity of E47/HEB. *Cancer Cell*. 5:587–596. doi:10.1016/j.ccr.2004.05.023

Olshen, A.B., E.S. Venkatraman, R. Lucito, and M. Wigler. 2004. Circular binary segmentation for the analysis of array-based DNA copy number data. *Biostatistics*. 5:557–572. doi:10.1093/biostatistics/kxh008

Park, S.T., G.P. Nolan, and X.H. Sun. 1999. Growth inhibition and apoptosis due to restoration of E2A activity in T cell acute lymphoblastic leukemia cells. *J. Exp. Med*. 189:501–508. doi:10.1084/jem.189.3.501

Reschly, E.J., C. Spaulding, T. Vilimas, W.V. Graham, R.L. Brumbaugh, I. Aifantis, W.S. Pear, and B.L. Kee. 2006. Notch1 promotes survival of E2A-deficient T cell lymphomas through pre-T cell receptor-dependent and -independent mechanisms. *Blood*. 107:4115–4121. doi:10.1182/blood-2005-09-3551

Schröck, E., and H. Padilla-Nash. 2000. Spectral karyotyping and multicolor fluorescence in situ hybridization reveal new tumor-specific chromosomal aberrations. *Semin. Hematol*. 37:334–347. doi:10.1016/S0037-1963(00)90014-3

Schwartz, R., I. Engel, M. Fallahi-Sichani, H.T. Petrie, and C. Murre. 2006. Gene expression patterns define novel roles for E47 in cell cycle progression, cytokine-mediated signaling, and T lineage development. *Proc. Natl. Acad. Sci. USA*. 103:9976–9981. doi:10.1073/pnas.0603728103

Sigvardsson, M., M. O'Riordan, and R. Grosschedl. 1997. EBF and E47 collaborate to induce expression of the endogenous immunoglobulin surrogate light chain genes. *Immunity*. 7:25–36. doi:10.1016/S1074-7613(00)80507-5

van Dongen, J.J., A.W. Langerak, M. Brüggemann, P.A. Evans, M. Hummel, F.L. Lavender, E. Delabesse, F. Davi, E. Schuuring, R. García-Sanz, et al. 2003. Design and standardization of PCR primers and protocols for detection of clonal immunoglobulin and T-cell receptor gene recombinations in suspect lymphoproliferations: report of the BIOMED-2 Concerted Action BMH4-CT98-3936. *Leukemia*. 17:2257–2317. doi:10.1038/sj.leu.2403202

van Doorn, R., R. Dijkman, M.H. Vermeer, J.J. Out-Luiting, E.M. van der Raaij-Helmer, R. Willemze, and C.P. Tensen. 2004. Aberrant expression of the tyrosine kinase receptor EphA4 and the transcription factor twist in Sézary syndrome identified by gene expression analysis. *Cancer Res*. 64:5578–5586. doi:10.1158/0008-5472.CAN-04-1253

Vermeer, M.H., R. van Doorn, R. Dijkman, X. Mao, S. Whittaker, P.C. van Voorst Vader, M.J. Gerritsen, M.L. Geerts, S. Gellrich, O. Söderberg, et al. 2008. Novel and highly recurrent chromosomal alterations in Sézary syndrome. *Cancer Res*. 68:2689–2698. doi:10.1158/0008-5472.CAN-07-6398

Willemze, R., E.S. Jaffe, G. Burg, L. Cerroni, E. Berti, S.H. Swerdlow, E. Ralfkiaer, S. Chimenti, J.L. Diaz-Perez, L.M. Duncan, et al. 2005. WHO-EORTC classification for cutaneous lymphomas. *Blood*. 105:3768–3785. doi:10.1182/blood-2004-09-3502

Yan, W., A.Z. Young, V.C. Soares, R. Kelley, R. Benezra, and Y. Zhuang. 1997. High incidence of T-cell tumors in E2A-null mice and E2A/Id1 double-knockout mice. *Mol. Cell. Biol*. 17:7317–7327.